

# On the influence of changes in the drag relation on surface wind speeds and storm surge forecasts

N. C. Zweers · V. K. Makin · J. W. de Vries · G. Burgers

Received: 4 March 2010 / Accepted: 19 September 2011  
© Springer Science+Business Media B.V. 2011

**Abstract** In this study it is investigated how uncertainties in the magnitude of the drag coefficient translate into uncertainties in storm surge forecasts in the case of severe weather. A storm surge model is used with wind stress data from a numerical weather prediction (NWP) model, to simulate several recent storms over the North Sea. For a fixed wind speed, the wind stress is linear in the drag coefficient. However, in the NWP model the wind speed is not fixed and increasing the drag in the NWP model results into reduced wind speeds. The results from simulations show that for given increase in the drag coefficient, the weakening of the 10-m wind field reduces the increase in the stress considerably. When the Charnock parameter is increased in the NWP model, the resulting relative changes in the wind stress are almost independent of the wind speed. This is related to the fact that the depth of the surface boundary layer depends on the wind speed. The ratio between relative changes in the wind stress and relative changes in the drag coefficient depends on the wind speed. For 10-m wind speeds larger than  $20 \text{ m s}^{-1}$  the ratio is 0.52; for lower wind speed criteria the ratio is somewhat larger ( $\sim 0.60$ ). Approximately 36% of the relative change in the drag coefficient translates into a relative change in the surge in stations at the Dutch coast. The relative increase in the storm surge is approximately 68% of the relative increase in the stress.

**Keywords** Wind stress · Drag coefficient · Storm surge · Uncertainties · Sensitivity

## 1 Introduction

Floods due to storm surges are a serious threat for The Netherlands. A significant part of the country (the coastal regions) is below mean sea level height. A large percentage of the population lives in these regions. The coastal area is also an important economic hotspot. There is industrial and shipping activity and the international harbour of Rotterdam is situated directly near the North Sea.

---

N. C. Zweers (✉) · V. K. Makin · J. W. de Vries · G. Burgers  
Royal Netherlands Meteorological Institute (KNMI), De Bilt, The Netherlands  
e-mail: zweers@knmi.nl

In the past there have been several dramatic storm surges that flooded the coastal area. The most recent one is the devastating storm surge in February 1953 that caused a massive flood in the southwestern part of the country. More than 1,800 casualties were reported and the damage to infrastructure was enormous. Since that storm, a great deal of work has been carried out in order to improve the safety of the coastal area and to prevent a similar disaster to occur again. Examples of these protective measures are the strengthening of dikes, but also the closure of the Eastern Scheldt in the southwestern part of the country with the Eastern Scheldt storm surge barrier. This is an open barrier that can be closed in case of a high surge. Several other storm surge barriers were built as well, like e.g. the Maeslantkering at Hoek van Holland.

Besides this kind of protective measures, accurate storm surge forecasting is another part of the safety issue. In operational storm surge forecasting the input comes from a numerical weather prediction model, usually in terms of a near-surface wind field. Then, this wind field is translated into surface stress by means of a drag coefficient  $C_D$ . This parameter, used to describe the transfer of momentum from air to water at the air-sea interface, is formulated as

$$C_D = \left( \frac{u_*}{U(z)} \right)^2, \tag{1}$$

with  $U(z)$  the horizontal wind speed at height  $z$  and  $u_*$  the friction velocity defined as  $u_* = \sqrt{\tau/\rho_a}$ , where  $\tau$  is the wind surface stress and  $\rho_a$  the density of air.

So far, observations leave a rather large uncertainty in the magnitude of the drag coefficient, which depends both on wind speed and the wave-state. This uncertainty can be found in numerous studies. We list here a few, e.g. Smith et al. (1992), Donelan et al. (1993), Johnson et al. (1998), Powell et al. (2003) and Drennan et al. (2005). Usually the 10-m drag coefficient is computed, corresponding with the 10-m wind speed  $U_{10}$ . As shown in the studies mentioned previously,  $C_{D10}$  increases approximately linearly with increasing  $U_{10}$  for  $U_{10}$  up to approximately  $30 \text{ m s}^{-1}$ . The uncertainty in  $C_{D10}$  grows with increasing wind speed.

For further analysis, the drag coefficient is based on the logarithmic wind profile (see Sect. 2) and aerodynamic roughness length. Based on dimensional analysis, Charnock (1955) suggested a relation for the aerodynamic roughness length for momentum  $z_0$ , given by

$$z_0 = z_* \frac{u_*^2}{g}, \tag{2}$$

with  $g$  the acceleration due to gravity and  $z_*$  known as the Charnock parameter. This formulation, referred to as the Charnock relation, is widely used in many atmospheric and oceanographic models and applications. Although Charnock originally suggested that the non-dimensional roughness  $z_*$  is a constant, the magnitude of the Charnock parameter depends on the atmospheric state through the wind speed as reported by Yelland and Taylor (1996), and also on the wave-state through the inverse wave age  $u_*/c_p$  (with  $c_p$  the phase speed of waves in the spectral peak) as shown in the previously mentioned studies, but with a high degree of uncertainty.

For convenience in atmospheric and oceanographic models the formulation in (2) is used with a constant value for the Charnock parameter. Consequently, the uncertainty in the drag coefficient is reflected by the value that is used for  $z_*$ : values differ in the range between 0.014 and 0.034.

In this study the aim is not to improve the accuracy of the drag coefficient computation. Our interest is in how uncertainties in the drag coefficient translate into uncertainties in storm surge forecasts. The focus is on situations of stormy weather, since the uncertainty in  $C_D$  is larger for higher wind speeds.

In storm surge models the drag coefficient is generally used as a tuning parameter. The wind stress that ultimately drives a storm surge model is linear in the drag coefficient. Naively, one would then expect that changes in the drag coefficient and the wind stress are the same. However, an increase (decrease) in sea drag will cause a decrease (increase) in the surface wind. Hence, the changes in drag and stress are not the same. To a good approximation the surge is linear in the stress. Hence, we are interested in the response of modelled storm surges to drag coefficient modification. Summarized, this paper will address the question: how do uncertainties in the magnitude of the drag coefficient translate into uncertainties in the modelled storm surge?

In this paper we use the storm surge model WAQUA/DCSM (Dutch Continental Shelf Model, see Gerritsen et al. 1995), which has been developed in a cooperation between the Dutch public works authority (Rijkswaterstaat), Deltares and the Royal Netherlands Meteorological Institute (KNMI). This model is used in The Netherlands for day-to-day forecasting of waterlevels along the Dutch coastline. The storm surge model is driven by the numerical weather prediction model HIRLAM<sup>1</sup> (High Resolution Limited Area Model), which is used for operational weather forecasting in The Netherlands.

The outline of the paper is as follows. In Sect. 2 the drag relation in the two models is discussed. Then, in Sect. 3 it is explained how we use HIRLAM and WAQUA/DCSM to simulate 4 storms that occurred in the North Sea area in the past few years. Details about these storms as well as the analysis of our data are briefly discussed. In Sect. 4 the results are presented. We end with conclusions and a discussion.

## 2 Stress and drag coefficient in HIRLAM and WAQUA/DCSM

For operational storm surge forecasting, WAQUA/DCSM is driven by surface pressure fields and 10-m wind fields ( $U_{10}$ ) from the numerical weather prediction model HIRLAM. The computation of  $U_{10}$  in HIRLAM is based on the constant flux layer approximation for wind stress. The wind stress, denoted by  $\tau$ , is computed in HIRLAM according to the traditional bulk relation

$$\tau = \rho_a C_D U_L^2 \quad (3)$$

with  $C_D$  the drag coefficient in HIRLAM according to (1) and  $U_L$  is the wind speed at the lowest model level, which we designate by  $z = L$ .

Assuming a constant flux layer means that the wind stress in (3) is constant with height in the lowest model layer, below the level  $z = L$ . When neutral stratification is assumed, then the wind speed in this layer ( $z_0 \leq z \leq L$ ) is logarithmic with height:

$$U(z) = \frac{u_*}{\kappa} \ln \left( \frac{z}{z_0} \right) \quad (4)$$

with  $\kappa = 0.41$  the Von Karman constant and  $z$  the height above the surface. When  $U_L$ ,  $u_*$  and  $z_0$  are known, the wind speed  $U_{10}$  is obtained from (4).

<sup>1</sup> Information on HIRLAM is available at <http://hirlam.org/>.

A direct relation between the drag coefficient and the roughness length follows from (1) and (4). It should be mentioned that the model includes atmospheric instability according to Monin-Obukhov mixing length theory. However, this does not play a role for our analysis, since we are interested in high wind speeds.

The crucial parameter in (4) is  $z_0$ . In HIRLAM, the computation of  $z_0$  is based on the summation of two terms: roughness due to viscosity (for  $U_{10} < 5 \text{ m s}^{-1}$ ) and roughness due to the presence of short-gravity waves for higher wind speeds, described by the Charnock relation. Since we examine storm cases, viscous effects are neglected. Consequently,  $z_0$  is given by the Charnock relation in (2). In HIRLAM the standard value for  $z_*$  is 0.025.

The stress that ultimately drives the storm surge model is obtained by translating  $U_{10}$  into stress by using the bulk relation in WAQUA/DCSM, which is different from HIRLAM:

$$\tau = \rho'_a C'_D U_{10}^2, \tag{5}$$

with  $\rho'_a$  the near-surface density of air in WAQUA/DCSM and  $C'_D$  the 10-m drag coefficient in the storm surge model. The computation of  $C'_D$  is also based on the Charnock relation. However, in WAQUA/DCSM the value for the Charnock parameter is different:  $z_* = 0.032$ . Moreover, the near-surface density of air is different in the two models:  $\rho'_a$  in WAQUA/DCSM is a constant, while  $\rho_a$  in HIRLAM is computed with the gas law. This implies unequal drag coefficients in the two models, which causes a discontinuity in the stress at the surface and hence an inconsistency in the model coupling. To avoid this, in this study we use a consistent formulation for sea drag. To that end, we drive the storm surge model with the wind stress directly from HIRLAM, given in (3). In this scenario we experiment with the roughness formulation in HIRLAM, so that we can investigate the impact of uncertainties in the sea drag on the sensitivity in both the wind stress and storm surges. The common methodology and our approach are displayed in Fig. 1.

### 3 Methodology

#### 3.1 Simulations with HIRLAM and WAQUA/DCSM

The atmospheric model HIRLAM (version 7.2.3) is used to model 4 storm cases in the North Sea. Sea level pressure, the 10-m wind field and wind stress fields are produced on a

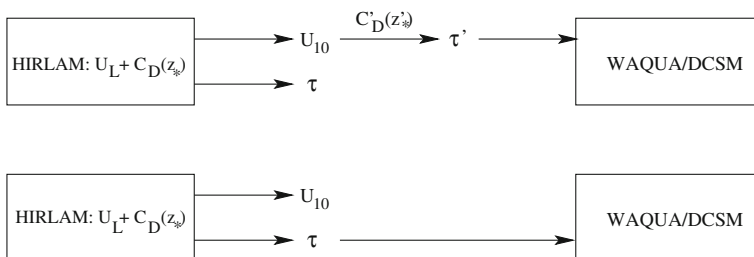


**Fig. 1** Traditional methodology (*upper graph*): transfer of the 10-m wind  $U_{10}$  with different drag coefficients, resulting into unequal stresses ( $\tau$  vs.  $\tau'$ ); methodology followed in this paper (*lower graph*): transfer of stress straight into the storm surge model

22 km resolution grid. The domain covers The Channel, the North Sea area and the eastern part of the North Atlantic Ocean. During the simulations, HIRLAM performs analyses every 6 h. From every analysis follows a 6-h period forecast. In this 6-h period the forecast data are stored every hour. The model uses lateral boundaries from the European Centre (ECMWF). The locations of these boundaries were chosen such that they did not affect the storms that were modelled inside the domain.

In order to examine the effect of uncertainties in sea drag, the storms are simulated several times with HIRLAM. Each time a different value for the Charnock parameter is used. At present, the default value in HIRLAM is 0.025. The values used for  $z_*$  are, respectively, 0.018, 0.022, 0.025, 0.028, 0.031, 0.033 and 0.036. These are realistic values for  $z_*$  and the values used in HIRLAM in the past are in this range of values. With the wind stress and the 10-m wind field, a 10-m drag coefficient  $C_{D10}$  is defined according to the constant flux layer approximation:

$$C_{D10} = \frac{\tau}{\rho_a U_{10}^2}. \tag{6}$$

With results from the different simulations, the response in  $\tau$  and  $C_{D10}$  is computed with respect to the reference scenario, in which  $z_* = 0.018$ . Regarding the response in  $C_{D10}$ , changes in  $\rho_a$  are ignored.

The 2D storm surge model WAQUA/DCSM is based on the shallow water equations. The model computes depth averaged currents and sea level heights for the North Sea area on a grid with 8 km resolution. In Fig. 2 the domain of the storm surge model is presented. The domain is smaller than the HIRLAM domain, which extends more north- and westwards. Based on 10-min intervals the model gives sea level height and surge.

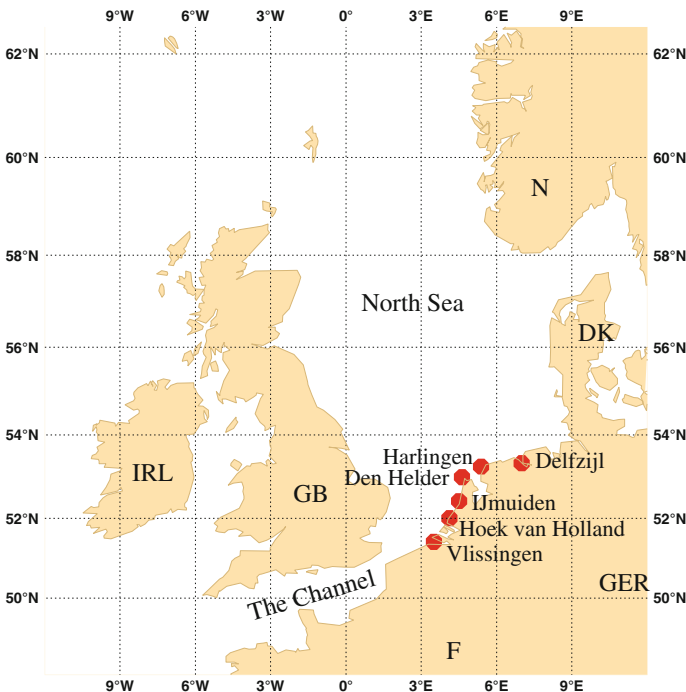


**Fig. 2** Domain of the storm surge model WAQUA/DCSM. The locations of six main stations are shown

Corresponding to the HIRLAM simulations with each a different  $z_*$ , each storm case is modelled several times with WAQUA/DCSM.

In the HIRLAM simulations, data assimilation is applied during the model analyses. The storm surge model uses the analyses data and +1h, ..., +5h forecast data from the HIRLAM simulations; the +6h forecast data overlaps the analyses and is therefore not used. For operational use, the storm surge model uses a Kalman filter for data assimilation of sea level observations. In this study, however, no data assimilation is applied in WAQUA/DCSM. The reason for this is that we want to avoid the impact of data assimilation on the modelled surge so that to each different  $z_*$  the modelled surge is an independent dataset. The length of the runs with the storm surge model is 4–5 days for each storm for each HIRLAM dataset.

### 3.2 Data selection

The response in wind stress and 10-m drag coefficient, denoted by  $\delta\tau/\tau$  and  $\delta C_{D10}/C_{D10}$ , respectively, are only computed in case of large  $U_{10}$ ; if in the reference scenario in grid points  $U_{10} > 20 \text{ m s}^{-1}$ , then  $\delta\tau/\tau$  and  $\delta C_{D10}/C_{D10}$  are computed. This is a reasonable criterion (see Sect. 3.3).

Regarding the uncertainty in the storm surge model outcome, we examine the response in the so-called *skew* surge, denoted by  $h_s$ . The surge simply is the difference between sea level height and astronomical tide at the same time in the tidal cycle. The *skew* surge is defined as the difference between highest (lowest) total sea level height and highest (lowest) water level due to astronomical tide in the same tidal cycle. We focus on the modelled skew surge in six main (coastal) stations for operational storm surge forecasting: Vlissingen and Hoek van Holland (south-western part of the Dutch coastline), IJmuiden and Den Helder (western part) and Harlingen and Delfzijl (northern part).

Furthermore, we only compute the skew surge response, denoted by  $\delta h_s/h_s$ , if the skew surge for a station is higher than 1.0 m in the reference scenario. The response in the relatively low skew surges in the datasets would otherwise become too large, hence dominating the results. During the storms, the (skew) surge typically is 1.0 m and often higher (see Table 1 in Sect. 3.3).

Eventually, we relate the surge response  $\delta h_s/h_s$  to the drag and stress response ( $\delta C_{D10}/C_{D10}$  and  $\delta\tau/\tau$ ). This is not straightforward, since wind speeds of a variety of locations and times are responsible for causing the high surge along the coastline. In general, the wind speed near and along the coastline was  $\sim 20 \text{ m s}^{-1}$  or higher, before and around the time of the high surges. Therefore, it is reasonable to relate the skew surge response to the  $\delta C_{D10}/C_{D10}$  dataset for  $U_{10} > 20 \text{ m s}^{-1}$ . However, since lower wind speeds might have contributed to the surge as well, the effect of using the  $\delta C_{D10}/C_{D10}$  dataset for  $U_{10} > 15 \text{ m s}^{-1}$  is also examined.

### 3.3 The storm cases

Four recent storms are studied: the 01 November 2006, 11–12 January 2007, 18–19 January 2007 and 08–09 November 2007 storms. These storms are characterized by high (skew) surges measured along the Dutch coastline (see Table 1).

The November cases were both storms over the North Atlantic Ocean south of Iceland that propagated towards Norway and Denmark. These storms caused very strong winds from north to northwest in the North Sea area ( $\sim 20\text{--}25 \text{ m s}^{-1}$ ) and along the Dutch coastline ( $\sim 15\text{--}20 \text{ m s}^{-1}$ ). The combination of such a strong northerly atmospheric flow

**Table 1** Observed skew surges higher than 1.0 m per station for the 01 Nov 2006 (A), 11–12 Jan 2007 (B), 18–19 Jan 2007 (C) and 08–09 Nov 2007 storm (D), during both low- and high-water (units are cm)

|   | Vlissingen | Hoek van Holland | IJmuiden | Den Helder | Harlingen | Delfzijl |
|---|------------|------------------|----------|------------|-----------|----------|
| A | +137       | +143             | +163     | +120       | +110      | +106     |
|   | +150       | +137             | +136     | +164       | +160      | +196     |
|   |            |                  |          | +125       | +227      | +348     |
|   |            |                  |          |            | +148      | +161     |
| B | +152       | +134             | +131     | +176       | +135      | +169     |
|   |            |                  | +163     | +154       | +211      | +248     |
|   |            |                  |          |            | +157      | +153     |
|   |            |                  |          |            | +103      | +101     |
| C | +167       | +109             | +122     | +117       | +170      | +198     |
|   |            |                  |          | +172       | +225      | +170     |
|   |            |                  |          |            | +101      | +118     |
|   |            |                  |          |            |           |          |
| D | +143       | +189             | +202     | +116       | +168      | +103     |
|   | +228       | +175             | +155     | +195       | +241      | +208     |
|   | +109       | +123             | +123     | +147       | +174      | +271     |
|   |            |                  |          | +109       | +122      | +220     |
|   |            |                  |          |            | +128      |          |

with the long fetch is the most ideal scenario for having a high surge along the Dutch coastline. During both storms the surge was high along the entire Dutch coastline. During the 2007 storm the Maeslantkering at Hoek van Holland had to be closed, which was the very first time ever in storm conditions since its construction. But the surge was highest along the Northern coastline. In fact, during the 2006 storm, a historical high-water record for the entire Dutch coastline was established in Delfzijl.

The two January cases were south-western storms. Such storms are dangerous mainly over land, but occasionally they induce a high surge. In these two cases the surge was high, especially along the northern coastline. The reason for this was a strong south-westerly wind ( $\sim 20\text{--}25 \text{ m s}^{-1}$ ) that amplified the northward propagating tidal wave flow, followed by a strong north-westerly wind ( $\sim 15\text{--}20 \text{ m s}^{-1}$ ), due to the storm moving eastward.

### 3.4 Data analysis

Our analysis starts from (6). Disregarding changes in the near-surface density, a change in roughness  $\delta z_*$  translates into a change in stress  $\delta\tau$  according to

$$\frac{\delta\tau}{\tau} = \frac{\delta C_{D10}}{C_{D10}} + 2 \frac{\delta U_{10}}{U_{10}}. \tag{7}$$

Our first interest is in the relation between  $\delta\tau/\tau$  and  $\delta z_*/z_*$ . As mentioned in Sect. 1, increasing the drag coefficient will result into a weakening of the wind field, which will reduce the increase in the stress considerably. In order to find out how large the impact of the change in the wind field is on the wind stress response, we calculate how much the stress changes if we change  $z_*$  and keep the wind speed  $U_{10}$  constant. This means that we solve (7) without the second term on the right-hand side. The response in  $C_{D10}$  is computed according to

$$\delta C_{D10} = \frac{\partial C_{D10}}{\partial z_0} \delta z_0. \tag{8}$$

Using the formulation for the logarithmic wind profile and the fact that  $z_0 = z_* \cdot \tau / \rho_a g$ , the relative change in the stress can be expressed in terms of  $\delta z_* / z_*$ . Then, one obtains

$$\left. \frac{\delta \tau}{\tau} \right|_{U_{10}} = \frac{\beta}{1 - \beta} \frac{\delta z_*}{z_*}, \tag{9}$$

with  $\beta = [2 / \ln(10 / z_0)] \propto \sqrt{C_{D10}}$ .

This equation is solved iteratively, for several fixed  $U_{10}$ . The results are compared with the wind stress response in HIRLAM, and the impact of changes in the wind field on the wind stress response are clarified.

In the general case that  $U_{10}$  is not constant, we relate  $\delta \tau / \tau$  in HIRLAM to  $\delta C_{D10} / C_{D10}$ . To that end, we define a parameter  $\gamma$  based on (7):

$$\frac{\delta \tau}{\tau} = \gamma \frac{\delta C_{D10}}{C_{D10}}. \tag{10}$$

Our second interest is in how the storm surge response  $\delta h_s / h_s$  relates to the drag response  $\delta C_{D10} / C_{D10}$ . The relative change in the surge in a particular coastal station is the response to changes in the stress field over a range of times. Therefore,  $\delta h_s / h_s$  is related to  $\langle \delta C_{D10} / C_{D10} \rangle$ , which is an average value over the entire domain during the entire model run, with  $\delta C_{D10} / C_{D10}$  selected on the 10-m wind speed (see Sect. 3.2). Hence, we examine a parameter  $\gamma'$  that we define according to

$$\left\langle \frac{\delta h_s}{h_s} \right\rangle = \gamma' \left\langle \frac{\delta C_{D10}}{C_{D10}} \right\rangle. \tag{11}$$

Finally, in a similar way we also relate  $\delta h_s / h_s$  directly to the averaged wind stress response, i.e. the increase in the wind stress averaged over the entire HIRLAM domain and during the entire simulation.

## 4 Results

### 4.1 Sensitivity of the wind stress and the drag coefficient

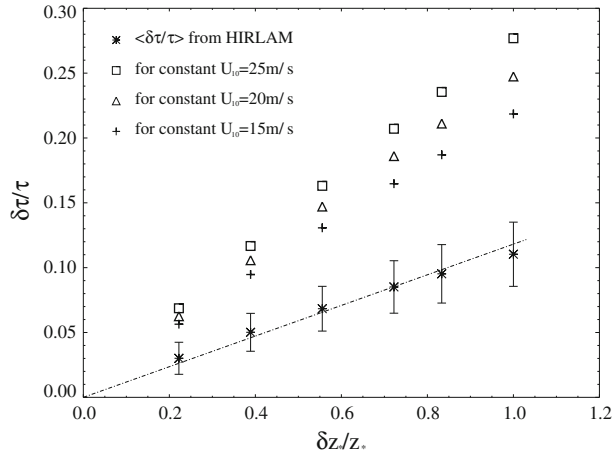
The results from the individual storms were very similar, which allowed us to combine the data. Therefore, the results are presented as one dataset. In Fig. 3 the relative change in the wind stress is presented as a function of the relative change in the Charnock parameter  $z_*$ , with respect to the  $z_* = 0.018$  scenario. The results from the HIRLAM simulations (for  $U_{10} > 20 \text{ m s}^{-1}$ ) are shown as well as the results from the case in which we change  $z_*$  and keep the 10-m wind speed unchanged (see Sect. 3.4). Results of the latter are shown for the case of  $U_{10} = 15, 20$  and  $25 \text{ m s}^{-1}$ . For the HIRLAM results, we present  $\langle \delta \tau / \tau \rangle \pm \sigma_\tau$ , i.e. mean values and the interval of one standard deviation.

For the given changes in  $z_*$ , the dashed-dotted line corresponds to the best fit for the data and is given by  $(\delta \tau / \tau) = 0.12 \cdot (\delta z_* / z_*)$ . The magnitude of  $\sigma_\tau$  is approximately 20% of  $\langle \delta \tau / \tau \rangle$ ; for the smallest change in  $z_*$  this number is larger.

As can be seen in Fig. 3, the increase in the wind stress in HIRLAM is much smaller than the increase in wind stress if the wind speed would not change. This indicates a significant (systematic) weakening in the 10-m wind field. For large increase in  $z_*$  the wind



**Fig. 3** Relative change in the wind stress ( $\delta\tau/\tau$ ) versus relative change in the Charnock parameter ( $\delta z_*/z_*$ ). HIRLAM data are shown for  $U_{10} > 20 \text{ m s}^{-1}$ : asterisks indicate  $\langle\delta\tau/\tau\rangle$ , bars indicate  $\pm \sigma_\tau$ . The symbols square, triangle and plus represent  $\langle\delta\tau/\tau\rangle$  for unchanged  $U_{10}$  of 25; 20; 15  $\text{m s}^{-1}$  respectively

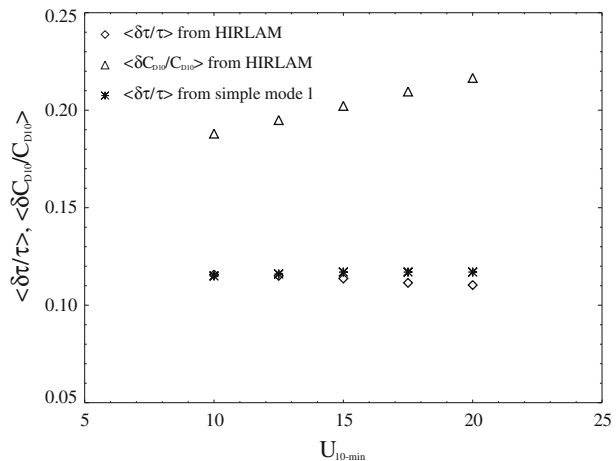


stress would increase by  $\sim 25\%$  if  $U_{10}$  is not changed; due to the weakening of the wind field in the NWP model, the response of the wind stress is approximately 10%.

Comparing the HIRLAM wind stress results for  $U_{10} > 20 \text{ m s}^{-1}$  with results for lower wind speed criteria, we find that the relative change in the wind stress only weakly depends on the  $U_{10}$  criterion. For the relative change in the 10-m drag coefficient this is not the case. Our results indicate that for large  $U_{10}$  the larger increase in  $C_{D10}$  is compensated by a larger decrease in the wind speed, which results into a response in the wind stress that is almost independent of the magnitude of  $U_{10}$ . In Fig. 4 we show the relative changes in stress and 10-m drag coefficient from HIRLAM as a function of the  $U_{10}$  criterion in the case of making  $z_*$  twice as large. As can be seen, the relative change in the 10-m drag coefficient increases with increasing 10-m wind speed, while the response in the wind stress in HIRLAM is almost independent on the 10-m wind speed.

The result that the increase in the stress is almost independent on the 10-m wind speed criterion is related to the fact that the surface boundary layer depth depends on the magnitude of the wind field: if the wind speed at the top of the surface boundary layer is larger, then the surface boundary layer is deeper. With a very simple model that includes

**Fig. 4** Averaged values of the relative change in the wind stress ( $\langle\delta\tau/\tau\rangle$ ) and the relative change in the 10-m drag coefficient ( $\langle\delta C_{D10}/C_{D10}\rangle$ ) from HIRLAM and the relative change in the stress from the simple model (see text) as a function of minimum 10-m wind ( $U_{10-\text{min}}$ ). The corresponding change in  $z_*$  here is from 0.018 to 0.036



this property we find that the response of the wind stress in HIRLAM indeed weakly depends on  $U_{10}$ . In this simple model, the wind speed at the top of the surface boundary layer  $h$  equals the geostrophic wind speed  $u_{\text{geo}}$ , and the surface stress is computed as a function of the wind speed  $u_{\text{geo}}$  and the Charnock parameter  $z^*$ . The model equations are given by

$$U(z) = \frac{u_*}{\kappa} \ln\left(\frac{z}{z_0}\right), \tag{12}$$

$$U(z = h) = u_{\text{geo}}, \tag{13}$$

$$h = c \frac{u_*}{f}, \tag{14}$$

where (14) is based on Ekman boundary layer height scaling (see e.g. Geernaert and Plant 1990), in which  $f$  is the Coriolis parameter ( $\mathcal{O}(10^{-4})$ ) and  $c$  is a constant, and  $z_0$  follows from (2). For  $c$ , we used a value of 0.15.

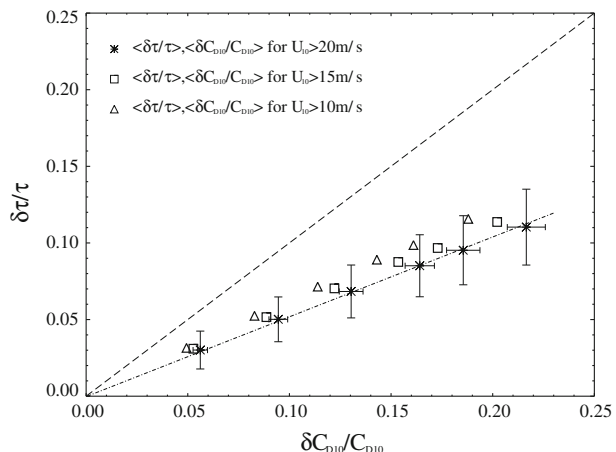
By increasing the value of  $z^*$  for fixed  $u_{\text{geo}}$ , the stress increases, the height of the surface boundary layer increases and the 10-m wind speed decreases. Using the same values for  $z^*$  as in the HIRLAM simulations, the stress is calculated for several values for  $u_{\text{geo}}$ . Again,  $\delta\tau/\tau$  is computed with respect to  $z^* = 0.018$ .

As shown in Fig. 4, the results from the simple model show that the relative increase in the stress is indeed almost independent on the 10-m wind speed. The figure shows that there is a clear resemblance between the stress response from HIRLAM and the relative change in stress from the simple model. Doing the same experiment with the simple model again, however, with a fixed value for the height  $h$ , we do not find this resemblance; then, the relative increase in the stress becomes slightly larger for higher wind speeds.

In Fig. 5, we present the change in the wind stress as a function of the change in the 10-m drag coefficient. For  $U_{10} > 20 \text{ m s}^{-1}$  we show  $[\langle\delta\tau/\tau\rangle \pm \sigma_\tau]$  and  $[\langle\delta C_{D10}/C_{D10}\rangle \pm \sigma_{C_{D10}}]$ ; we also show  $\langle\delta\tau/\tau\rangle$  and  $\langle\delta C_{D10}/C_{D10}\rangle$  for  $U_{10} > 15; 10 \text{ m s}^{-1}$ .

Due to the change in  $U_{10}$ , the changes in stress and drag coefficient are not the same, for any  $U_{10}$  criterion we impose. For  $U_{10} > 20 \text{ m s}^{-1}$  the best fit for the data (see (10)) is given by

**Fig. 5** Relative change in wind stress ( $\delta\tau/\tau$ ) versus relative change in 10-m drag coefficient ( $\delta C_{D10}/C_{D10}$ ). Asterisks indicate mean values, bars indicate  $\pm\sigma_{\tau,C_{D10}}$  ( $U_{10} > 20 \text{ m s}^{-1}$ ); squares and triangles represent mean values for  $U_{10} > 15; 10 \text{ m s}^{-1}$  respectively. The dashed line only illustrates equal responses in stress and drag coefficient. The dashed-dotted line represents the best fit (15) to the data



$$\frac{\delta\tau}{\tau} = 0.52 \frac{\delta C_{D10}}{C_{D10}}. \tag{15}$$

For lower wind speeds, the effect of the wind field weakening on  $\gamma$  reduces. For  $U_{10} > 15 \text{ m s}^{-1}$  we find  $\gamma = 0.57$ ; for  $U_{10} > 10 \text{ m s}^{-1}$  we find  $\gamma = 0.62$ . The magnitude of  $\sigma_{C_{D10}}$  is  $\sim 1\text{--}5\%$  of  $\langle \delta C_{D10}/C_{D10} \rangle$ .

### 4.2 Sensitivity of storm surge

As mentioned in Sect. 3.2 we relate the relative change in the skew surge to the response in the drag coefficient for  $U_{10} > 20 \text{ m s}^{-1}$ . To that end, we use average values for  $\delta C_{D10}/C_{D10}$  for the HIRLAM domain. We examine the effect of the wind speed criterion, by computing  $\gamma'$  in (11) also for  $U_{10} > 15 \text{ m s}^{-1}$ .

In Fig. 6 we present  $[\langle \delta h_s/h_s \rangle \pm \sigma_{h_s}]$  and  $[\langle \delta C_{D10}/C_{D10} \rangle \pm \sigma_{C_{D10}}]$  for  $U_{10} > 20 \text{ m s}^{-1}$ ; mean values are shown for  $U_{10} > 15 \text{ m s}^{-1}$ . The best fit for the data corresponds with

$$\left\langle \frac{\delta h_s}{h_s} \right\rangle = 0.36 \left\langle \frac{\delta C_{D10}}{C_{D10}} \right\rangle. \tag{16}$$

The magnitude of  $\sigma_{h_s}$  is approximately 15% of  $\langle \delta h_s/h_s \rangle$ . For  $U_{10} > 15 \text{ m s}^{-1}$  we find  $\gamma' = 0.38$ . Hence, the value for  $\gamma'$  is not severely affected by the choice for the threshold for  $U_{10}$ .

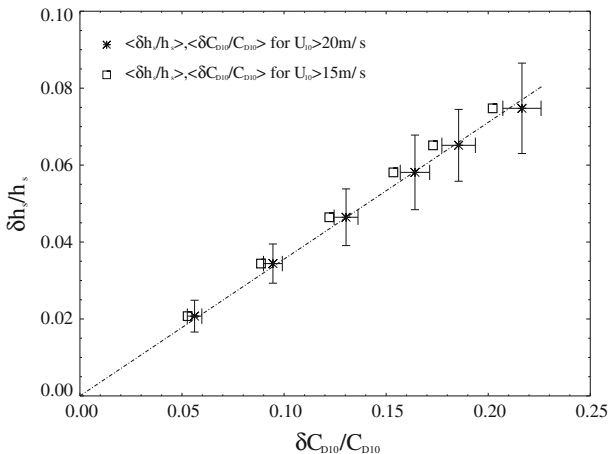
When we relate the response in the storm surge directly to the response in the wind stress, the best fit to our data is given by

$$\left\langle \frac{\delta h_s}{h_s} \right\rangle = 0.68 \left\langle \frac{\delta\tau}{\tau} \right\rangle, \tag{17}$$

where  $\langle \delta\tau/\tau \rangle$  represents the relative increase in stress averaged over the HIRLAM domain. The ratio in (17) weakly depends on the  $U_{10}$  criterion on the stress data; for  $U_{10} > 15 \text{ m s}^{-1}$  we find a ratio of 0.67.

To the best approximation, 68% of the increase in the stress translates into an increase in the skew surge along the coastline. However, this result is based on averaged values for the increase in the stress and one should notice that the result in (17) comes with quite some spread in the data, for both the response in the skew surge as well as the stress. Moreover,

**Fig. 6** Relative change in skew surge ( $\delta h_s/h_s$ ) versus relative change in 10-m drag coefficient ( $\delta C_{D10}/C_{D10}$ ). Asterisks indicate mean values, bars indicate  $\pm \sigma_{h_s, C_{D10}}$  ( $U_{10} > 20 \text{ m s}^{-1}$ ); squares represent mean values for  $U_{10} > 15 \text{ m s}^{-1}$ . The dashed line represents the best fit (16) to the data



the ratio is based on the surge in coastal stations only. When we consider areas that are located more seaward, then the ratio becomes smaller. This is partly caused by the fact that the surge is lower in these areas than the 1.0 m criterion we imposed.

The results in (16) and (17) are based on averaged values of the relative changes in  $C_{D10}$  and  $\tau$ , respectively, in which we averaged for the entire HIRLAM domain for the entire duration of the simulations. In order to examine whether the results in (16) and (17) are dependent on this way of averaging, the relative changes in  $C_{D10}$  and  $\tau$  were also computed for the storm surge model domain, for the entire duration of the simulations. Moreover, we also computed averaged values for a shorter time period that corresponds with the time period in which each storm was active in the North Sea area. This was done for both the entire HIRLAM domain and the storm surge model domain. The results from these three other methods of averaging indicate that the results in (16) and (17) are robust; the values for  $\gamma'$  for different  $U_{10}$  do not change considerably (less than 5%) when averaging over a different domain and/or different time period.

## 5 Conclusions and discussion

Several storms have been modelled with a storm surge model that was driven by wind stress data from a numerical weather prediction (NWP) model. In this NWP model the magnitude of the drag coefficient was modified in order to examine how uncertainties in sea drag translate into uncertainties in the storm surge through changes in the wind stress. Changes in the drag coefficient were forced by changing the value of the Charnock parameter in the roughness formulation. As discussed in Zweers et al. (2010), changes in the drag at very high wind speeds that cannot be represented by a change in the Charnock parameter have similar effects on storm intensity as shown here.

From the results follows the important concept that an increase in the drag coefficient in a numerical weather prediction model results into a decrease of the magnitude of the near-surface wind field. Hence, when the 10-m wind field is used for storm surge forecasting, then the fine-tuning of the 10-m drag coefficient in the storm surge model to obtain realistic storm surge forecasts could lead to an inconsistency in the model coupling. This implies that one should take great care in treating the drag coefficient as a tuning parameter in storm surge modelling. Using wind stress instead of wind speed as input for a storm surge model, one can avoid the conversion of wind speed into stress. Then, one should focus on the accuracy of the surface roughness formulation and proper computation of the wind stress in an atmospheric model, which can be used then in a storm surge model. When the fine-tuning of the 10-m drag coefficient in a storm surge model is done consistently, then our results show that the relative change in the storm surge is only approximately 35% of the relative change in the 10-m drag coefficient.

For given increase in the drag coefficient, the systematic weakening of the near-surface wind field reduces the increase in the stress considerably. For a given change in the Charnock parameter, we find that the relative increase in the 10-m drag coefficient becomes larger with increasing 10-m wind speed, while the relative increase in the stress is almost independent of the 10-m wind speed. We have been able to reproduce this result with a rather simple model that is based on known empirical facts, which confirms that our result is robust. The fact that the relative increase in the stress is almost independent of the 10-m wind speed is related to the fact that the depth of the surface boundary layer increases with increasing wind speed. The response in the stress is smaller than the response in the 10-m drag coefficient. In fact, in the case of storm conditions we find that the relative

increase in the stress is approximately 50% of the relative increase in the 10-m drag coefficient. This is considered as advantageous; although there is uncertainty in the magnitude of the drag coefficient for storm conditions, the possible errors that are made in computing the drag coefficient are suppressed in the stress response. And particularly for the modelling and forecasting of severe storms, the uncertainty in the drag formulation is largest.

**Acknowledgments** The authors acknowledge the support by the Netherlands Organization for Scientific Research (NWO), project number 816.01.011, and the Office of Naval Research (ONR), Grant N000 14-08-1-0609.

## References

- Charnock H (1955) Wind stress on a water surface. *Q J R Meteorol Soc* 81:639–640
- Donelan MA, Dobson FW, Smith SD, Anderson RJ (1993) On the dependence of sea surface roughness on wave development. *J Phys Oceanogr* 23(9):2143–2149
- Drennan WM, Taylor PK, Yelland MJ (2005) Parameterizing the sea surface roughness. *J Phys Oceanogr* 35(5):835–848
- Geernaert GL, Plant WJ (1990) Surface waves and fluxes. Kluwer Dordrecht, The Netherlands
- Gerritsen H, De Vries H, Philippart M (1995) The Dutch continental shelf model. In: Lynch D, Davies A (eds) Quantitative skill assessment for coastal ocean models. Coastal and estuarine studies. American Geophysical Union, vol 47, pp 425–467
- Johnson HK, Højstrup J, Vested HJ, Larsen SE (1998) On the dependence of sea surface roughness on wind waves. *J Phys Oceanogr* 28(9):1702–1716
- Powell MD, Vickery PJ, Reinhold TA (2003) Reduced drag coefficient for high wind speeds in tropical cyclones. *Nature* 422(6929):279–283
- Smith SD, Anderson RJ, Oost WA, Kraan C, Maat N, De Cosmo J, Katsaros KB, Davidson KL, Bumke K, Hasse L et al (1992) Sea surface wind stress and drag coefficients: the HEXOS results. *Boundary Layer Meteorol* 60(1):109–142
- Yelland M, Taylor PK (1996) Wind stress measurements from the open ocean. *J Phys Oceanogr* 26:541–558
- Zweers NC, Makin VK, de Vries JW, Burgers G (2010) A sea drag relation for hurricane wind speeds. *Geophys Res Lett* 37:L21811. doi:[10.1029/2010GL045002](https://doi.org/10.1029/2010GL045002)